

Dual-Awareness Attention for Few-Shot Object Detection

Tung-I Chen, Yueh-Cheng Liu, Hung-Ting Su, Yu-Cheng Chang, Yu-Hsiang Lin, Jia-Fong Yeh, Winston H. Hsu
National Taiwan University

Abstract—While recent progress has significantly boosted few-shot classification (FSC) performance, few-shot object detection (FSOD) remains challenging for modern learning systems. Existing FSOD systems follow FSC approaches, ignoring the issues of spatial misalignment and vagueness in class representations, and consequently result in low performance. Observing this, we propose a novel Dual-Awareness Attention (DAnA) mechanism that can adaptively generate query-position-aware (QPA) support features and guide the detection networks precisely. The generated QPA features represent local information of a support image conditioned on a given region of the query. By taking the spatial relationships across different images into consideration, our approach conspicuously outperforms previous FSOD methods (+6.9 AP relatively) and achieves remarkable results even under a challenging cross-dataset evaluation setting. Furthermore, the proposed DAnA component is flexible and adaptable to multiple existing object detection frameworks. By equipping DAnA, conventional object detection models, Faster R-CNN and RetinaNet, which are not designed explicitly for few-shot learning, reach state-of-the-art performance in FSOD tasks.

Index Terms—Deep learning, object detection, visual attention, few-shot object detection.

I. INTRODUCTION

As a newly emerging and rapidly growing research topic, few-shot object detection (FSOD) has the great potential in real-world applications. Unlike conventional object detectors, FSOD models could be adapted to novel domains with only few samples, saving the onerous and time-consuming process to re-collect numerous annotated data of the upcoming tasks.

Previous attempts at FSOD are heavily based on the concepts and techniques proposed in few-shot classification (FSC). For instance, the techniques of building category prototypes [1], [2], ranking similarity between inputs [3], [4] and concatenating feature maps [5], [6] have all been adopted in FSOD. However, while recent progress has boosted FSC accuracy, state-of-the-art FSOD models, such as [4], still have considerable performance gap in comparison to generic object detection models. In our experiments, we show that existing FSOD approaches suffer low performance even though they are tested on base (training) categories (Tab. II). Motivated by the observations, it is worthy to analyze the deficiencies in current FSOD frameworks.

FSOD is a challenging task due to the complicated composition of queries (image to be tested) and various representations of supports (few examples). In FSC, both the support and query images are close-ups of specific objects with simple photography composition. The queries in FSOD, however,

contain multiple objects of various categories, so it would be more challenging and intractable to capture the shared contexts among instances. Moreover, FSOD models have to not only perform classification but also estimate the spatial location of each object. In comparison to FSC, FSOD requires more effective techniques to measure query-support correlations.

Previous works remain an implicit assumption that those techniques leveraged in FSC can be directly applied to FSOD without causing serious issues. In this work, we list three potential issues in existing FSOD methods (see Fig. 1). Prior attempts [2], [7], [8], [6], [9], [10] widely employed (a) global average pooling to enhance computational efficiency, but it will inevitably undermine the spatial information carried in support images. In addition, while (b) convolution-based attention operations [11], [6] can establish query-support correlations with efficiency, the spatial misalignment of objects across intra-class images has been ignored. Moreover, (c) previous methods [2], [7], [8], [6], [4], [9] follow FSC to construct class-specific representations by directly averaging the features of few images, which would probably lead to biased and unclear category information [12]. The aforementioned issues might not be severe in FSC due to the relatively simple problem setting, yet FSOD is a much more complicated task requiring specific and accurate contextual information to localize and identify instances.

To verify the motivation, we explore a pilot study with the hypothesis: *If the spatial variability and biased support features are not crucial in FSOD, the choice of support images would not severely affect the performance.* In the experiment, four well-trained models are tested on the same query set 100 times, but the given support sets will be different in each iteration. For fair comparison, the given supports will be identical among the four methods. As illustrated in Fig. 2, the gaps between the highest and lowest results of the three baseline methods are large (up to 4.4 AP), while our method achieves the firmest performance across different given supports. Such results substantiate our assumption that the selection bias of support images has significant influence on the results of previous methods. However, it is infeasible to always ensure high-quality supports in real-world scenarios. In this work, we demonstrate that higher performance and robustness can be achieved by addressing the issues illustrated in Fig. 1.

To address the problems in Fig. 1, we propose *Dual-Awareness Attention* (DAnA) mechanism comprised of *Background Attenuation* (BA) block and *Cross-image Spatial Attention* (CISA) block. The BA block is inspired by the

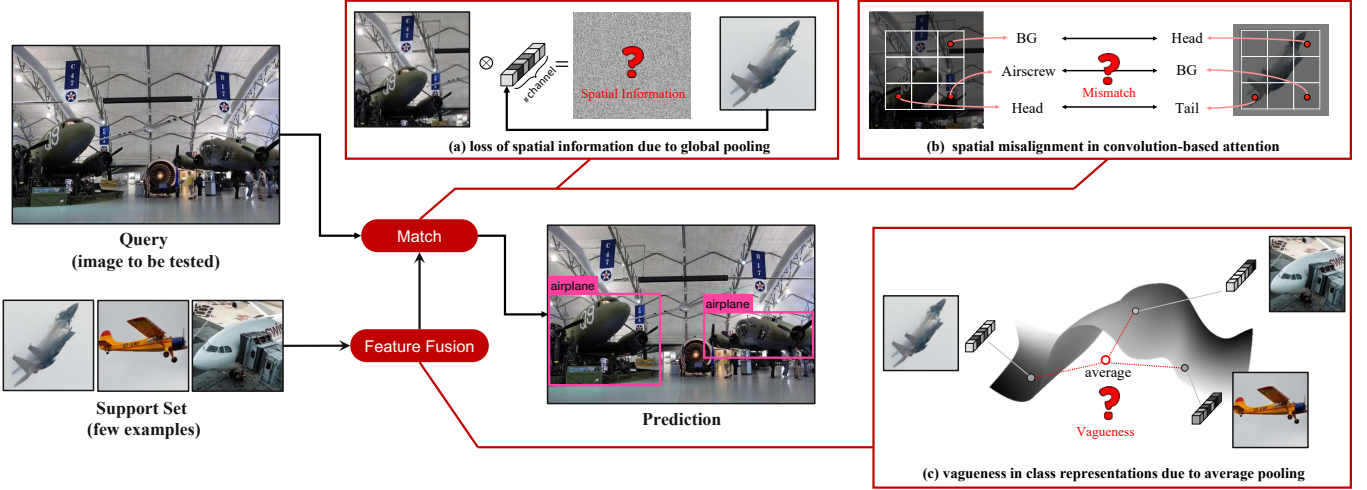


Fig. 1: Illustration of the few-shot object detection task and the issues that might hinder the performance (a-c). (a) Previous works achieve computational efficiency by encoding support images into global feature vectors, leading to a severe loss of spatial information and local contexts. (b) The convolution-based attention techniques have difficulty in modeling the relationships across objects with varying spatial distributions. (c) Taking the mean features over support images as class-specific representations might lead to vagueness and bias in class information.

phenomenon called *wave interference*. Each feature vector ($1 \times 1 \times C$) of the high-level feature map ($H \times W \times C$) is considered as a *signal* of specific patterns that represent particular local contexts. In BA block, we leverage attention to aggregate a feature map into a one-dimensional vector that represents the most important information of that support image, and add this vector to each spatial location of the original feature map. If the local features are similar to the learned aggregation, those features will be more distinguishing after the addition. The features of backgrounds, on the other hand, will degenerate and could be easily recognized as irrelevant features by the following modules. The BA technique can be regarded as a softer attention process that undermines background features while preserves comprehensive foreground information.

To determine whether two objects belong to the same class, a human would first find out the most representative features of these objects (e.g., dog paws, bird wings) and then make the decision based on these features. Inspired by such a nature, we propose CISA block where the attention maps for support images are adaptable to different local contexts of a query. Specifically, support feature maps are transformed into query-position-aware (QPA) features, and each QPA feature vector represents specific local contexts of a support image. For each local region of the query, CISA provides customized QPA features of relevant support information. Those query regions having high responses with their QPA vectors should be identified as the target. (see Fig. 8).

By disentangling support images into QPA vectors, CISA breaks the physical restriction of Convolutional Neural Network (CNN) and provides a novel way to extract desired information from multiple support images irrespective of spatial distribution. Since those QPA vectors conditioned on the same position of the query represent information relevant to each other, taking the mean features across QPA vectors can avoid

the risk of resulting in vague class representations. By better exploiting support images, experiments show that our method has a significant improvement as the number of given support images increases (see Tab. II).

In this paper, we evaluate the models across multiple settings, including the multi-shot, multi-way, cross-domain, and episode-based evaluations. In Tab. I we show that our method significantly outperforms the strongest baseline [13] by 6.9 AP under the 30-shot setting. Furthermore, we are the first to conduct zero-shot evaluation for FSOD (Tab. II and Tab. III), where models are trained from the source domain and directly tested on the target domain without fine-tuning. The model size and inference speed of each method are reported as well, which have not been evaluated in previous papers. We also offer a comprehensive ablation study to demonstrate the impact of each proposed component.

Our main contributions can be summarized as follows:

- We point out the critical deficiencies in previous FSOD approaches that would lead to the lack of robustness and degenerated performance.
- We present a novel dual-awareness attention to attenuate undesired information and capture relevant contexts across images.
- We conduct comprehensive experiments to fairly assess each approach. Extensive experimental results manifest the effectiveness and robustness of the proposed methodology.

II. RELATED WORKS

A. Few-Shot Classification

Few-shot classification (FSC) has multiple branches, including the optimization-based and metric-based approaches. The optimization-based methods [14], [15], [16], [17], [18] aim to learn a good initialization parameter set that can swiftly be

adapted to new tasks within few gradient steps. The metric-based methods [3], [19], [1], [5], [12], [20], on the other hand, compute the distance between learned representations in the embedding space. The concept of prototypical representation [1] is widely adopted in FSC, which takes the mean feature over different support images as a class-specific embedding. Such a strategy is intuitive yet the data scarcity in few-shot scenarios might lead to biased prototypes and consequently hinder the performance [12]. To enhance the reliability of class representations, Tian *et al.* [20] leveraged pre-trained embedding and showed that using good representations is more effective than applying sophisticated meta-learning algorithms. Although the attempts have successfully boosted the performance of FSC, the progress of few-shot object detection (FSOD) is still in a very early stage. In this work, we explore novel attention mechanisms and significantly enhance the performance of FSOD.

B. Attention Mechanism

The attention modules were first developed in natural language processing (NLP) to facilitate machine translation [21], [22], [23]. Recently, inspired by the great success of Transformer [24], researchers start to explore the self-attention mechanism on computer vision (CV) problems [25], [26], [27], [28], [29], [30], attempting to break the physical restrictions of CNN. Wang *et al.* [25] presented a pioneering approach, Non-local (NL) Neural Networks, leveraging self-attention to capture long-range dependencies in an image. Hu *et al.* [31] adopted a self-attention function on channels, re-weighting features along the channel dimension. Following NL, [26] described the features as information flows that can be bidirectionally propagated; [28] showed that simplifying NL block does not deteriorate its ability but rather enhance the performance; recently, Yin *et al.* [32] succeeded in capturing better visual clues by proposing a disentangled NL block. Emami *et al.* [33] combined spatial attention with GAN to handle image-to-image translation tasks. Li *et al.* [34] explored attention in both spatial and temporal dimensions, improving the performance of video action detection.

The main differentiating factor between the proposed DAnA and aforementioned attention mechanisms is that DAnA can capture cross-image dependencies and interpret support images adaptively according to the given query. It would be plausible that the idea of DAnA can be applied to other research topics aiming to capture shared attributes among images with diverse backgrounds, viewpoints and illumination conditions [35], [36], [37], yet in this work we will emphasize the application in FSOD only.

C. Few-Shot Object Detection

Deep-learning-based object detectors have shown remarkable performance in many applications. Two-stage detectors [38], [39], [40], [41] are usually dominant in performance, and one-stage detectors [42], [43], [44], [45] are superior in run-time efficiency. Most modern object detectors are category-specific, which means they are incapable of recognizing objects of unseen categories. To explore generalized object

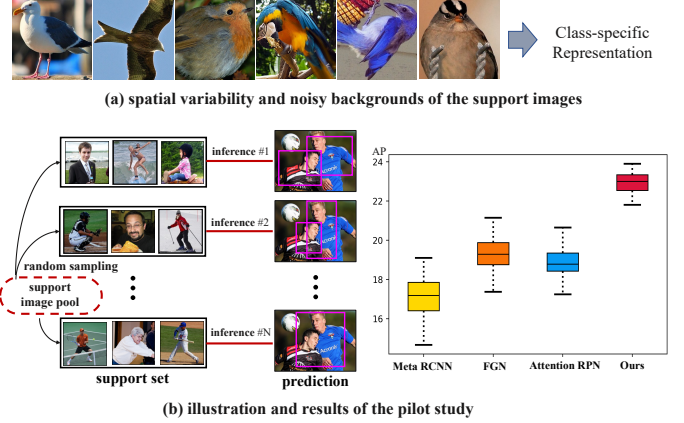


Fig. 2: The pilot study of model robustness. We explore an experiment to test whether the quality of support images would seriously influence FSOD results. The standard deviations of AP of the four methods are [0.72, 0.81, 0.68, 0.46] respectively, indicating that our method is effective in alleviating the selection bias of supports by only extracting crucial information.

detectors, previous attempts exploited transfer learning [46] and distance metric learning [2] to achieve quick adaption to novel domains. As recasting object detection problem into the few-shot learning paradigm, the idea of current methods could be somewhat similar to multiple-instance learning (MIL) [47], [48], [49]. For FSOD, we can also perceive a query image as a bag, aiming to identify the positive image patches in it by capturing the contexts relevant to given support images [47].

Recently, there is an important line of works encoding support images into global vectors, measuring the similarity between feature vectors and the ROI proposals inferred by detection networks [7], [8]. Following the spirit, [6] perceived the task as a guided process where support features are used to guide the object detection networks. Inspired by [11], Fan *et al.* [4] measured the correlations by regarding support images as kernels and performing a convolution-based operation over queries. Current works have a tendency to take mean features as class representations and measure cross-image correlations by either feature concatenation or element-wise product [8], [2], [6], [4]. We argue that these techniques will engender serious issues (illustrated in Fig. 1) in FSOD, degenerating the performance even on the seen (training) categories.

III. METHODOLOGY

A. Problem Definition

Let s be a support image and $\mathcal{S} = \{s_i\}_{i=1}^M$ be a support set that represents a specific category. An individual FSOD task can be formulated as $\mathcal{T} = \{(\mathcal{S}^1, \dots, \mathcal{S}^N), \mathcal{I}\}$, where \mathcal{I} is a query image comprised of multiple instances and backgrounds. Given \mathcal{T} , the model should detect all the objects in \mathcal{I} belonging to the target categories $\{\mathcal{S}^1, \dots, \mathcal{S}^N\}$. The object categories in a training dataset are divided into two disjoint parts: base classes \mathcal{C}^{base} and novel classes \mathcal{C}^{novel} . To train a FSOD model, a meta-training set $\mathcal{H}^{train} = \{\mathcal{T}_i\}_{i=1}^{|\mathcal{H}|}$ should be constructed, where all the bounding box annotations belong to

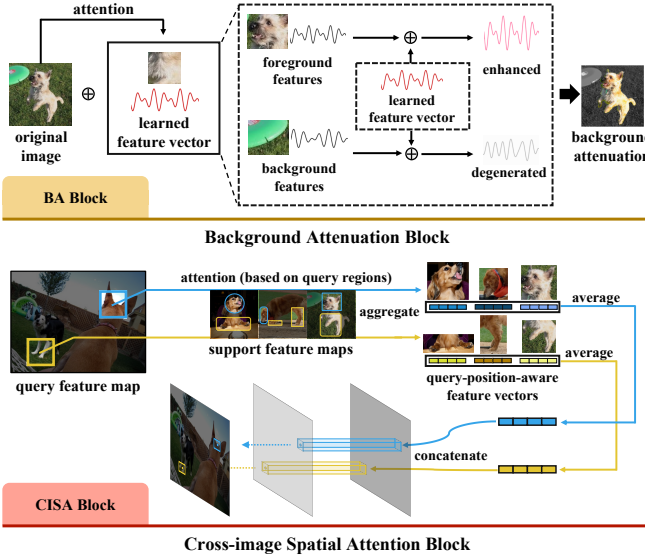


Fig. 3: Illustration of our proposed methods. In BA block, the learned aggregation is superimposed on the original feature map. The most discriminative features will be enhanced, while the features associated with backgrounds will degenerate. To better leverage support information, CISA block adaptively transforms feature maps into query-position-aware features conditioned on the local features of query images.

\mathcal{C}_{base} . Similarly, a meta-testing set \mathcal{H}^{test} is constructed where all the target objects belong to \mathcal{C}_{novel} . It is allowed to use a fine-tuning set $\mathcal{H}^{finetune}$ to fine-tune the model before evaluating on \mathcal{H}^{test} . However, in an N -way K -shot setting, only K box annotations of each novel category can be used to fine-tune the model [2], [7].

To summarize, the primary goal of FSOD is to leverage rich source-domain knowledge in \mathcal{H}^{train} to learn a model that can swiftly generalize to target domains where only few annotated data are available. Instead of only considering the features of \mathcal{I} , the model $f(\mathcal{I}|\mathcal{S})$ is trained to recognize objects conditioned on the given support information.

B. Dual-Awareness Attention

1) *Overview*: FSOD relies on limited support information to detect unseen objects in queries, and therefore we consider two important aspects: 1) The quality of support features, and 2) how to better construct correlations across the support and query images. Previous works [2], [7], [8], [6], [4], [9] condensed support feature maps into one-dimensional vectors by global pooling, and then measured correlations between the query and support with efficiency. Since feature maps have been transformed into vectors, the various spatial distributions of objects would not be a serious concern. However, we have been placed in a dilemma that applying global pooling will sacrifice local contextual information (Fig. 1 (a)), while abandoning global pooling indicates that the spatial misalignment across images should be tackled (Fig. 1 (b)). Additionally, it remains as a challenge to retrieve distinguishing information from limited support images without causing vagueness and

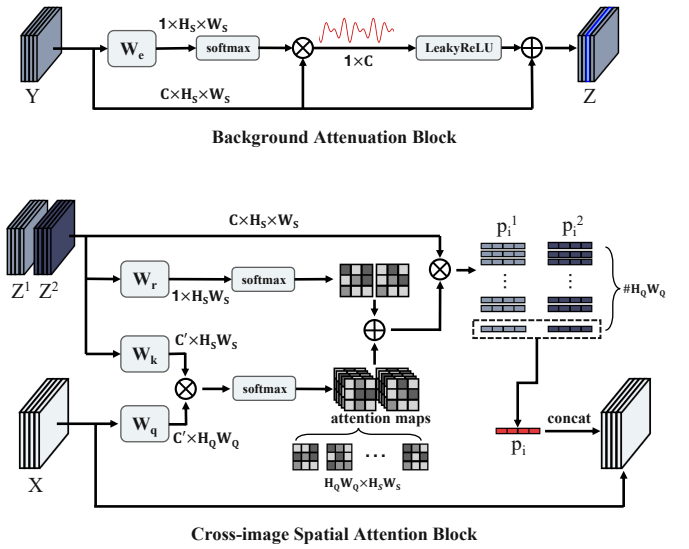


Fig. 4: Detailed structures of the two proposed modules. \otimes denotes matrix multiplication, while \oplus denotes broadcast element-wise addition; W denotes a learned weight matrix; Y and X are support and query feature maps respectively; Z^1 denotes the 1st feature map in a support set enhanced by BA block; p_i denotes the query-position-aware support feature corresponding to the i^{th} pixel of a query feature map X .

bias (Fig. 1 (c)). To resolve these issues, we propose two novel modules that can enhance the local contexts and extract customized support features according to queries.

2) *Background Attenuation Block*: It is infeasible to always ensure high-quality support images in real-world situations. Those irrelevant backgrounds would lead to considerable noise, inhibiting models from reaching robustness (see Fig 2). We propose a novel mechanism, *Background Attenuation* (BA), to undermine the undesired information in support images. The detailed structure of BA block is illustrated in Fig. 4, where a support image s and a query image \mathcal{I} are encoded into a support feature map $Y \in \mathbb{R}^{C \times H_S \times W_S}$ and a query feature map $X \in \mathbb{R}^{C \times H_Q \times W_Q}$ by a shared CNN backbone. In BA block, the feature map Y will be reshaped and transformed by a linear learnable matrix $W_e \in \mathbb{R}^{C \times 1}$. The process can be formulated as

$$\mathcal{A}_{BA}(y_i) = \sigma(W_e y_i) = \frac{\exp(W_e y_i)}{\sum_{j \in \Omega} \exp(W_e y_j)} \quad (1)$$

where $y_i \in \mathbb{R}^{1 \times C}$ denotes the feature vector at i^{th} pixel of Y ; Ω is the set of all pixel indices and σ is the softmax function applied along the spatial dimension. Thus, the learned aggregation of Y can be obtained by

$$G = \sum_{i \in \Omega} \mathcal{A}_{BA}(y_i) \cdot y_i. \quad (2)$$

Intuitively, $G \in \mathbb{R}^{1 \times C}$ should represent the most important parts of Y based on attention. However, we empirically discover that employing such an attention-based aggregation for denoising undermines the performance instead (see Tab. VI). By visualization, it can be observed that only few narrow regions of

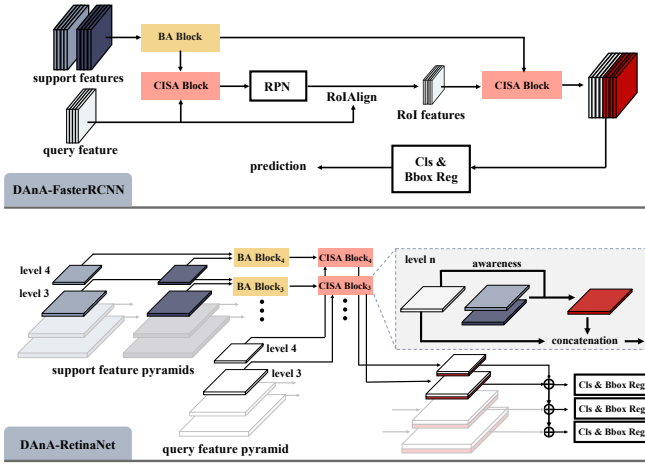


Fig. 5: The model architectures of DAnA-FasterRCNN and DAnA-RetinaNet. Our proposed components are flexible and can be easily combined with existing object detection frameworks which are not originally designed for FSOD.

support image contribute to the aggregated feature G . Such a naive attention process leads to a considerable loss of support information and would deteriorate the ability of models.

Based on the observation, we propose a much softer attention strategy to remove noise. In physics, *interference* phenomenon that two signals superpose to form a resultant signal of greater or lower amplitudes. Inspired by that, we regard each feature vector of Y as a C -dimensional signal, and superimpose the learned aggregation G on those signals

$$Z = Y + \alpha \cdot \text{LeakyReLU}(G) \quad (3)$$

where α is a constant hyper-parameter, and the nonlinear function is used to rectify the results. As illustrated in Fig. 3, if the original signals (*e.g.*, regions belonging to the dog) are aligned with G , the resultant signals will achieve higher amplitudes. In contrast, those signals associated with unrelated regions (*e.g.*, the Frisbee) will degenerate due to the huge difference with G . The BA block benefits the detection network by offering more discriminative support features to it.

In comparison to previous attention approaches, the idea of BA is different from [31], [27] that leveraged channel-wise attention to reweight feature maps along the channel dimension. Unlike [28] constructed heavy linear transformation matrices to reweight semantic dependencies, BA block is more efficient since $W \in \mathbb{R}^{C \times 1}$ is the only learnable weights in it.

3) *Cross-image Spatial Attention Block*: In practice, intra-class objects have a wide range of variations so it is usually challenging to retrieve unified and discriminative information from multiple support images. The core idea of Cross-image Spatial Attention (CISA) is to adaptively transform ordinary support features into query-position-aware (QPA) features that represent specific semantic information. The first step of CISA is similar to QKV attention [24], where we transform X and Z into the query and key embeddings $\mathcal{Q} = W_q X, \mathcal{K} = W_k Z$ by learned weight matrices $W_q, W_k \in \mathbb{R}^{C \times C'}$. The correlation

scores between the query and support can then be measured by

$$\delta(X, Z) = \sigma((\mathcal{Q} - \mu_{\mathcal{Q}})^\top (\mathcal{K} - \mu_{\mathcal{K}})) \quad (4)$$

where $\mu_{\mathcal{Q}}$ and $\mu_{\mathcal{K}}$ are the averaged embedding values over all pixels; the softmax function σ is performed over the spatial dimension. In addition, we add a simplified self-attention term [28] in CISA because we assume the attention should be based on not only query-support correlations but also the support itself. Consequently, the CISA attention function is formulated as

$$\mathcal{A}_{\text{CISA}}(X, Z) = \delta(X, Z) + \beta \cdot W_r Z \quad (5)$$

where β is a constant coefficient; $W_r \in \mathbb{R}^{C \times 1}$. Note that the output of $\mathcal{A}_{\text{CISA}}(X, Z)$ has the shape of $H_Q W_Q \times H_S W_S$, which can be regarded as multiple support attention maps $\in \mathbb{R}^{H_S \times W_S}$ conditioned on different spatial locations of the query feature map $\in \mathbb{R}^{H_Q \times W_Q}$. The QPA feature vector can therefore be generated by

$$p_i = \sum_{j \in \Omega} \mathcal{A}_{\text{CISA}}(X, Z)_{ij} \cdot z_j \quad (6)$$

where Ω denotes all pixel indices of the support feature map. The equation shows that all the vectors of Z are adaptively weighted and aggregated into a vector $p_i \in \mathbb{R}^{1 \times C}$ according to each query position i (resolve Fig. 1 (a)). If there are K -shot images in a support set $\{s\}^K$, we can directly average the generated QPA features map $P \in \mathbb{R}^{C \times H_Q \times W_Q}$

$$P = \frac{1}{K} \sum_{k=1}^K P_k \quad (7)$$

without the concern of entangled representations, because those QPA vectors p_i^k of the same entry will represent relevant contextual information by taking the same query position i into consideration (resolve Fig. 1 (c)). CISA also breaks the physical restriction of spatial alignment since the QPA feature map P is no longer an ordinary support feature map but a combination of multiple aggregated vectors p_i^k (resolve Fig. 1 (b)). To apply the DAnA component to existing object detection frameworks, we can simply combine the output P with X and send them to the modules such as the region proposal network (RPN) to propose regions having high responses with the given supports.

C. Model Architecture

It is worth mentioning that the output of DAnA module has the same spatial size as the original query feature map, and can be concatenated as $PX \in \mathbb{R}^{2C \times H_Q \times W_Q}$. Thus, the proposed method can be easily applied to various existing object detection networks, including two-stage and one-stage methods (Fig. 5). In our experiments, we choose Faster R-CNN [40] and RetinaNet [42] as the backbones to verify the effectiveness of DAnA mechanism. For DAnA-FasterRCNN, one CISA block is leveraged before RPN, and the other CISA block is applied in the second stage which takes cropped ROI features as queries. For DAnA-RetinaNet, we apply both BA and CISA modules to each level of the feature pyramids.

Method	10shot		30shot	
	AP	AP ₇₅	AP	AP ₇₅
TFA w/cos [50]	10.0	9.3	13.7	13.4
Feature Reweighting [7]	5.6	4.6	9.1	7.6
Meta R-CNN [8]	8.7	6.6	12.4	10.8
Attention RPN [4]	11.1	10.6	-	-
IFSOD [9]	5.1	-	-	-
MPSR [51]	9.8	9.7	14.1	14.2
Viewpoint Estimation [13]	12.5	9.8	14.7	12.2
DAnA-FasterRCNN (Ours)	18.6	17.2	21.6	20.3

TABLE I: The performance on novel categories of COCO. All the models are trained on base categories and then fine-tuned on a small set of novel samples (e.g., 10 shots of each category). After fine-tuning, models will be evaluated on the novel classes. “-”: no reported results.

Furthermore, we follow the modification applied in [4], replacing the multi-class classification output with the binary one. Since the pipeline of FSOD can be regarded as a matching process based on given supports, we assume the binary output could better fit the problem scenarios where an instance will be either positively or negatively labelled. The rest details of the proposed model architectures remain the same as the original Faster R-CNN and RetinaNet.

IV. EXPERIMENTS

A. Implementation Details

By default, we employ the pretrained ResNet50 as the feature extractor, and the batch size is set to 32 for all the experiments. All the models including baselines were implemented in Pytorch [52] on a workstation with 4 NVIDIA Tesla V100. The shorter side of query images is resized to 600 pixels, while the longer side is cropped at 1000. Each support image will be zero-padded and then resized to a square image of 320×320 . The embedding dimension C' in the weight matrices W_q and W_k is a quarter of the number of original feature channels C . The constant coefficients α and β of the proposed modules are 0.5 and 0.1 individually. For those models based on Faster R-CNN [40], we adopt SGD with an initial learning rate of 0.001, which decays into 0.0001 after 12 epochs; the four anchor scales are $[60^2, 120^2, 240^2, 480^2]$ and the three aspect ratios are $[0.5, 1.0, 2.0]$; the momentum and weight decay coefficients are set to 0.9 and 0.0005. For DAnA-RetinaNet, we construct a pyramid with levels $P3$ through $P7$ (P^l has resolution 2^l lower than the input) and adopt Adam with a learning rate of 0.00001. We adopt the two-way contrastive training strategy, which is first proposed in [4], to train the baselines and our models.

B. Experimental Settings

1) *Dataset*: In the experiments, we leverage the challenging Microsoft COCO 2017 [53] benchmark for evaluation. COCO has 80 object classes, consisting of a training set with 118,287 images and a validation set with 4,952 images. Generally, the validation split of COCO will serve as the testing data due to the fact that the testing split is not released to the public.

We define the 20 COCO categories intersecting with PASCAL VOC [54] as the novel classes, while the rest 60 categories covered by COCO but not VOC to be the base classes.

2) *FSOD Training*: Following the paradigm of meta-learning, the training data are organized into *episodes*. Each episode contains one or more support sets, a query image and corresponding ground truth annotations. Unlike the queries in FSC, a query image in FSOD might contain multiple objects of different categories. Therefore, in each training step we will choose one of the object categories as the target. The corresponding support set will be offered and the model should learn to detect the target objects conditioned on the given support information. Note that all the annotations belonging to the novel categories have been removed in order to prevent models from peeking at the novel task.

3) *FSOD Evaluation*: Generally, N -way K -shot in the few-shot paradigm indicates that we can use K images of each novel category to adapt the models before testing. However, we found that previous works adopted different evaluation settings and fine-tuning protocols, leading to the ambiguity in comparison. For instance, since a query in FSOD might consist of multiple objects of different categories, Kang *et al.* [7] defined that there should be only K box annotations of each category in the fine-tuning set, while Chen *et al.* [46] adopted the protocol of collecting K query images of each category to fine-tune their models. To thoroughly evaluate the proposed method, in Tab. I we follow the widely-used protocol in [7] and compare our results with those works adopting the same evaluation setting. In addition, we further carry out experiments under the proposed zero-shot protocol (Tab. II, III, IV, V), where we do NOT leverage any labelled data of the target domain to fine-tune the models. We expect that a well-developed few-shot object detector can be applied to target domains as long as a few of support images are given without the costly data re-collection and bounding box annotating process. Due to the issue illustrated in Fig. 2, we will ensure the given support sets are the same across different methods in our experiments.

C. Generic FSOD Protocol

The performance of each method under the general FSOD protocol is reported in Tab. I. In this table, we comply with the evaluation protocol widely used in previous works and compare our results with the numbers reported in previous papers. As we have discussed in Sec. IV-B1, the models will be tested on the 20 novel categories of COCO and these classes remain unseen in the training. To test the generalization ability, only $K = 10, 30$ bounding box annotations per novel class can be used to fine-tune the models. Under such a challenging setting, Tab. I shows that our method surpasses previous approaches by a large margin. By equipping with DAnA, Faster R-CNN conspicuously outperforms the strongest baseline [13] by 6.1 and 6.9 AP under the 10-shot and 30-shot fine-tuning protocol respectively.

D. Zero-shot FSOD Protocol

In this section, we evaluate the models under a more challenging zero-shot protocol. Note that the word “zero-shot”

Method	Novel Categories									Base Categories									# parameters	FPS		
	AP			AP ₅₀			AP ₇₅			AP			AP ₅₀			AP ₇₅						
	N/A			N/A			N/A			34.3			58.3			35.6						
Faster R-CNN [†] [40]	1shot	3shot	5shot	1shot	3shot	5shot	1shot	3shot	5shot	1shot	3shot	5shot	1shot	3shot	5shot	1shot	3shot	5shot	4.76×10^7	31		
# Way	1way	3way	5way	1way	3way	5way	1way	3way	5way	1way	3way	5way	1way	3way	5way	1way	3way	5way				
# Given Supports	1shot	3shot	5shot	1shot	3shot	5shot	1shot	3shot	5shot	1shot	3shot	5shot	1shot	3shot	5shot	1shot	3shot	5shot				
Meta R-CNN [†] [8]	8.7	11.1	11.2	19.9	25.3	25.9	6.8	8.5	8.6	27.3	28.6	28.5	50.4	52.5	52.3	27.3	28.4	28.2	4.76×10^7	28		
FGN [†] [6]	8.0	10.5	10.9	17.3	22.5	24.0	6.9	8.8	9.0	24.7	25.5	26.9	44.3	46.4	47.6	25.0	25.5	27.4	1.48×10^8	23		
Attention RPN [†] [4]	8.7	10.1	10.6	19.8	23.0	24.4	7.0	8.2	8.3	20.6	22.4	23.0	37.2	40.8	42.0	20.5	22.2	22.4	1.03×10^8	21		
DAnA-FasterRCNN	11.9	14.0	14.4	25.6	28.9	30.4	10.4	12.3	13.0	27.8	29.4	32.0	46.3	50.6	54.1	27.7	30.3	32.9	1.42×10^8	24		

TABLE II: The 1-way, zero-shot evaluation on COCO. All the few-shot methods are trained on base categories and then tested on novel domains without fine-tuning. Note that Faster R-CNN [40] serves as the upper bound of few-shot methods, which is trained and evaluated under the generic object detection protocol. Compared with prior works, the relative mAP improvement of our method is up to 49% on novel categories. We also reduce the performance gap between generic and few-shot object detection approaches. The model size and inference speed are reported as well. [†]: re-implemented results.

Method	Novel Categories									Base Categories									# parameters	FPS		
	AP			AP ₅₀			AP ₇₅			AP			AP ₅₀			AP ₇₅						
	1way	3way	5way	1way	3way	5way	1way	3way	5way	1way	3way	5way	1way	3way	5way	1way	3way	5way				
# Way	1way	3way	5way	1way	3way	5way	1way	3way	5way	1way	3way	5way	1way	3way	5way	1way	3way	5way				
# Given Supports	5shot			5shot			5shot			5shot			5shot			5shot						
Meta R-CNN [†] [8]	11.2	11.0	10.2	25.9	25.2	23.4	8.6	8.6	8.0	28.5	27.4	26.2	52.3	50.8	48.7	28.2	26.8	25.7				
FGN [†] [6]	10.9	10.8	9.6	24.0	23.4	21.2	9.0	9.1	8.1	26.9	25.1	23.6	47.6	45.4	42.4	27.4	25.3	23.8				
Attention RPN [†] [4]	10.6	9.8	9.0	24.4	22.8	20.8	8.3	7.9	7.3	23.0	21.3	20.2	42.0	39.8	37.7	22.4	20.6	19.7				
DAnA-FasterRCNN	14.4	13.7	12.6	30.4	28.2	25.9	13.0	12.4	11.3	32.0	31.0	29.5	54.1	52.2	49.9	32.9	31.7	30.3				

TABLE III: The multi-way, zero-shot evaluation on COCO. Under the N -way setting, the given support set will be comprised of N categories and the model should detect all the objects that belong to any of those presented categories.

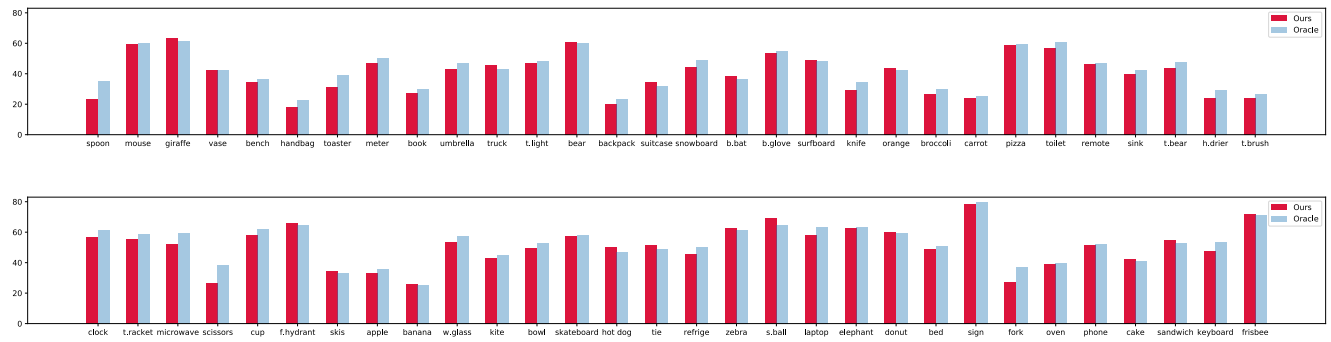


Fig. 6: Visualization of the AP on each base (training) category of COCO. We suggest that a well-developed few-shot object detector should be comparable to the generic object detector on the categories that have been seen during the training. This figure demonstrates that our model indeed achieves comparable performance on training categories and even surpass the oracle on some particular classes.

here is not referred to the zero-shot learning paradigm [55], but the fact that we do not take any instance of the novel domain to fine-tuned models after they have been trained on the base domain. To analyze each method under the unified zero-shot protocol, we re-implement three methods: Meta R-CNN [8], FGN [6] and Attention RPN [4] as the baselines, which shares the same backbone detector, Faster R-CNN, with our approach. Note that we have slight modifications on these frameworks: 1) we replace the multi-class classification output with the binary one as explained in III-C, and 2) we adopt the two-way contrastive training strategy [4] which is empirically effective in our experiments. Under such an experimental setting, the only difference between the baselines and the proposed DAnA-FasterRCNN will be the employed attention components, so the impact of different attention mechanisms can be precisely analyzed.

As we discussed in Sec. IV-B3, all the methods under the proposed zero-shot protocol are evaluated without

fine-tuning. Tab. II shows the results predicted with different numbers of given supports. With 5-shot support images, DAnA-FasterRCNN outperforms FGN and Attention RPN by 3.5/6.4/4.0 and 3.8/6.0/4.7 mAP respectively on AP/AP₅₀/AP₇₅ metrics. It is worth mentioning that our method achieves the most significant improvement as the shot increases, manifesting that DAnA can better retrieve the information carried within support images by transforming them into QPA features.

Without being fine-tuned on the novel domain, a well-developed FSOD model is supposed to perform well on base classes under the zero-shot protocol. We report the performance on base classes as well, and use an oracle model to quantify the performance gaps between the generic object detector and FSOD models. The oracle, Faster R-CNN [40], is trained on 60 base classes and its performance on base classes is regarded as the upper bound of the four FSOD models in Tab. II. It can be observed that previous works suffer

Method	Novel Categories			Base Categories		
	AP			AP		
# Way		1way		1way		
# Given Supports	1shot	3shot	5shot	1shot	3shot	5shot
Meta R-CNN [†] [8]	7.8	9.0	9.3	33.7	34.8	35.1
FGN [†] [6]	6.7	7.4	7.7	30.5	31.2	32.1
Attention RPN [†] [4]	6.8	7.4	7.7	23.7	26.6	27.2
DAnA-RetinaNet	9.1	10.3	11.5	36.5	36.9	37.2
DAnA-FasterRCNN	10.0	11.6	11.9	36.5	38.1	38.6

TABLE IV: The results of PASCAL2COCO evaluation. All the models are trained on PASCAL VOC 2007 and tested on COCO 2014. The base categories here denote the 20 classes shared between PASCAL VOC and COCO, while the novel categories are the other 60 classes in the COCO dataset.

Method	Novel Categories					
	AP			AP ₇₅		
# Way		1way		1way		
# Given Supports	1shot	3shot	5shot	1shot	3shot	5shot
Meta R-CNN [†] [8]	14.7	17.0	17.4	13.1	15.0	15.2
FGN [†] [6]	14.9	16.7	17.9	13.8	15.5	16.8
Attention RPN [†] [4]	15.0	17.1	18.1	13.7	15.4	16.2
DAnA-RetinaNet	16.6	18.8	19.5	15.5	17.7	18.4
DAnA-FasterRCNN	17.9	21.3	21.6	17.0	20.2	20.4

TABLE V: Following [2], we construct class-balanced episodes from COCO for evaluation. Note that we compare the two proposed models based on different backbone detectors. Though the two-stage few-shot object detectors generally achieve better performance than the one-stage, we show that RetinaNet [42] equipping with DAnA significantly outperforms two-stage baselines.

an obvious performance drop on base categories, while our approach has the smallest performance gap with the oracle. The results substantiate our argument that DAnA is effective in capturing query-support correlations irrespective of object categories. Note that we also provide the model sizes and inference speed in Tab. II, showing that applying our proposed component only leads to little additional cost in comparison to prior approaches.

In Tab. III, we further evaluate each method under the multi-way evaluation setting. Under the multi-way setting, the model must detect more than one object category conditioned on the given support set. Suppose there are M categories in a query image, we randomly select N classes from them to formulate an N -way FSOD task. In the case of $N > M$, we will sample $N - M$ classes which do not exist in that query and then append them to those M categories to form an N -way task. Under the multi-way setting, our method also significantly outperforms the baselines.

Fan *et al.* [6] evaluated models under the COCO2VOC setting, where models are trained on the 60 COCO categories disjoint with VOC, and then tested on PASCAL VOC [54]. In this work, we consider a more challenging setting termed PASCAL2COCO, where models are trained on PASCAL VOC 2007 and tested on the COCO benchmark. The 60 categories disjoint with VOC will serve as the novel categories, which is opposite to the previous experiments. The results of such cross-domain experiments are reported in Tab. IV.

In Tab. V, we follow the same zero-shot protocol but con-

Architecture with RPN	Average Pooling across QPA features	Denoising		Combination		Novel Categories	
		Mask	BA	product	concat	AP	AP ₅₀
a	✓					✓	12.6 26.9
b	✓	✓				✓	13.5 28.4
c	✓	✓	✓			✓	11.4 24.2
d	✓	✓	✓	✓		✓	10.5 22.8
e	✓	✓	✓	✓	✓	✓	11.5 23.8
f	✓	✓	✓	✓	✓	✓	13.8 28.8

TABLE VI: The results of ablations. (a,b) shows the effectiveness of using QPA features. (b,f) and (d,f) show that using BA block indeed improves the performance. (e,f) shows that RPN plays an important role in fully representing the advantages of DAnA.

struct the test dataset in a manner borrowed from FSC. Instead of directly testing on COCO validation split, we prepare 500 random evaluation episodes according to the episode-based evaluation protocol defined in RepMet [2]. In each episode, take N -way K -shot evaluation for example, there will be K support images for each of the N categories, and there are 10 query images for each category. Consequently, there will be $K \times N$ support images and $10 \times N$ query images in each episode, and models are tested on the episodes.

In Tab. IV and Tab. V, we compare DAnA-FasterRCNN with another proposed framework, DAnA-RetinaNet, to evaluate the effectiveness and impact of DAnA on different backbone detectors. Generally, those two-stage few-shot object detectors [50], [8], [4], [51], [13] with region proposal network (RPN) have higher performance than one-stage [7], [9] networks (see Tab. I). However, DAnA-RetinaNet, which is based on the one-stage network, can outperform those two-stage baseline methods. The results suffice to show the effectiveness and dexterity of DAnA. Nonetheless, it seems that the use of feature pyramids does not help DAnA-RetinaNet reach better results. Without RPN, detectors will enumerate a nearly exhaustive list of potential object locations and have to classify each of them. Moreover, the class-imbalance issue is extremely serious in DAnA-RetinaNet because only few foregrounds of the target category should be positively labeled. Based on the experiments, we suppose that RPN plays a deep role in fully presenting the advantages of DAnA.

E. Ablations

We conduct the ablation study in Tab. VI, analyzing the impact of each proposed component.

a) Whether CISA block can better utilize multiple support images: In Sec. III-B3, we argue that the vagueness in class representations can be addressed by averaging across query-position-aware (QPA) features, so we investigate the improvement brought by such a feature aggregation strategy in ablation experiments. The ablation (a, b) substantiates our argument that leveraging QPA features is more effective than directly performing averaging pooling across features of multiple support images.

b) Why not just denoise by soft attention: To attenuate the noise in support images, it is intuitive to directly learn a soft attention mask that reweights the importance of each pixel. The ablations (b, f) and (d, f) show the effectiveness of employing BA block, where “Mask” denotes that we leverage



Fig. 7: At training, the model has never seen the novel categories, including bird, car, dog, person, motorcycle, bicycle, etc. However, given different support examples, our model is capable of recognizing unseen target objects in the query image. The last row represents the failure case where the model confuses a bicycle with a motorcycle.

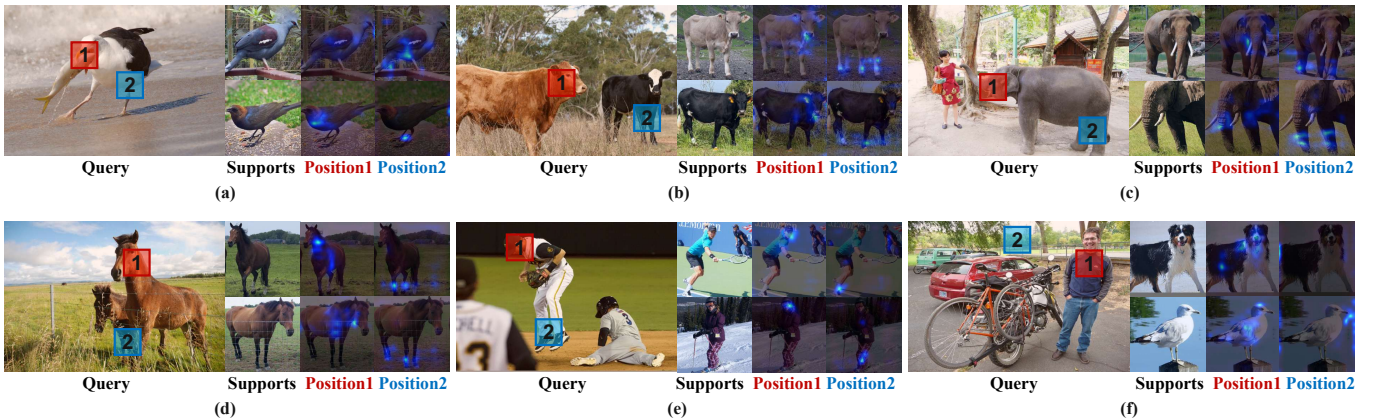


Fig. 8: For each query image, we consider two different regions (colored in red and blue) and visualize their corresponding support attention maps. The CISA module is capable of capturing the semantic correspondence between the query and support (e.g., the head or legs of an animal). (f) represents the special case where neither of the support categories exists in the query image.

CNN to learn a soft attention mask and perform element-wise product between the mask and the support image. The proposed BA block can attenuate background noise yet preserve crucial information.

c) *Should the resultant QPA features be concatenated or multiplied with the query feature map?*: Since QPA support feature maps have the same size as query feature maps, they can be combined by either feature map concatenation or element-wise product. According to (b, c), we conclude that concatenation is a better strategy for measuring correlations.

d) *The evaluation on adopting different backbone models*: We have reported the quantification results of the two proposed models, DAnA-FasterRCNN (with RPN) and DAnA-RetinaNet (without RPN) in Tab. IV and V. In the ablations, we compare these two models again to further analyze the impact of DAnA on different backbone networks, where

“RPN” denotes adopting Faster R-CNN as the backbone. The results suggest that RPN indeed plays a deep role in FSOD since it is capable of alleviating the serious class-imbalance issue by effectively reducing the number of redundant region proposals. Without RPN, the advantages of DAnA could not be fully presented.

F. Visualizations

The examples of few-shot object detection are demonstrated in Fig. 7. In FSOD, the prediction is dependent on the object category of the given support set. Notably, all the target instances in Fig. 7 belong to the novel classes, so the model has never been trained to recognize these objects. However, given few support images, the proposed model is capable of recognizing and locating the instances. The last row of Fig. 7

presents a failure case where a motorcycle is given yet the bicycle in the query is detected.

We also visualize the cross-image spatial attention (CISA) in Fig. 8. The CISA module is capable of capturing the semantic correspondence between the query and support. Take (e) for example, given the head (colored in red) or the feet of a human (colored in blue), the attention maps will highlight the head or the feet areas of the support images. The result (f) represents the case that neither of the support categories exists in the query image, which shows that if there is no corresponding contextual information, CISA has a tendency to highlight the most distinguishing components that can best describe an object.

V. CONCLUSION

In this work, we observed the problem of spatial misalignment and vague support information in the challenging few-shot object detection (FSOD) task. We propose a novel and effective Dual-Awareness Attention (DAnA) mechanism to tackle the problem. Our method is adaptable to both one-stage and two-stage object detection networks. DAnA remarkably boosts the FSOD performance on the COCO benchmark and reaches state-of-the-art results. We are excited to point out a new direction to solve FSOD tasks. We encourage future works to extend our method to other challenging tasks such as few-shot instance segmentation and co-salient object detection.

ACKNOWLEDGMENT

This work was supported in part by the Ministry of Science and Technology, Taiwan, under Grant MOST 110-2634-F-002-026. We benefit from NVIDIA DGX-1 AI Supercomputer and are grateful to the National Center for High-performance Computing.

REFERENCES

- [1] J. Snell, K. Swersky, and R. Zemel, “Prototypical networks for few-shot learning,” in *Advances in neural information processing systems*, 2017, pp. 4077–4087.
- [2] L. Karlinsky, J. Shtok, S. Harary, E. Schwartz, A. Aides, R. Feris, R. Giryes, and A. M. Bronstein, “Repmet: Representative-based metric learning for classification and few-shot object detection,” in *Proceedings of the IEEE Conference on Computer Vision and Pattern Recognition*, 2019, pp. 5197–5206.
- [3] G. Koch, R. Zemel, and R. Salakhutdinov, “Siamese neural networks for one-shot image recognition,” in *ICML deep learning workshop*, vol. 2. Lille, 2015.
- [4] Q. Fan, W. Zhuo, C.-K. Tang, and Y.-W. Tai, “Few-shot object detection with attention-rpn and multi-relation detector,” in *Proceedings of the IEEE/CVF Conference on Computer Vision and Pattern Recognition*, 2020, pp. 4013–4022.
- [5] F. Sung, Y. Yang, L. Zhang, T. Xiang, P. H. Torr, and T. M. Hospedales, “Learning to compare: Relation network for few-shot learning,” in *Proceedings of the IEEE Conference on Computer Vision and Pattern Recognition*, 2018, pp. 1199–1208.
- [6] Z. Fan, J.-G. Yu, Z. Liang, J. Ou, C. Gao, G.-S. Xia, and Y. Li, “Fgn: Fully guided network for few-shot instance segmentation,” in *Proceedings of the IEEE/CVF Conference on Computer Vision and Pattern Recognition*, 2020, pp. 9172–9181.
- [7] B. Kang, Z. Liu, X. Wang, F. Yu, J. Feng, and T. Darrell, “Few-shot object detection via feature reweighting,” in *Proceedings of the IEEE International Conference on Computer Vision*, 2019, pp. 8420–8429.
- [8] X. Yan, Z. Chen, A. Xu, X. Wang, X. Liang, and L. Lin, “Meta-r-cnn: Towards general solver for instance-level low-shot learning,” in *Proceedings of the IEEE International Conference on Computer Vision*, 2019, pp. 9577–9586.
- [9] J.-M. Perez-Rua, X. Zhu, T. M. Hospedales, and T. Xiang, “Incremental few-shot object detection,” in *Proceedings of the IEEE/CVF Conference on Computer Vision and Pattern Recognition*, 2020, pp. 13 846–13 855.
- [10] W. Liu, C. Zhang, G. Lin, and F. Liu, “Crnet: Cross-reference networks for few-shot segmentation,” in *Proceedings of the IEEE/CVF Conference on Computer Vision and Pattern Recognition*, 2020, pp. 4165–4173.
- [11] L. Bertinetto, J. Valmadre, J. F. Henriques, A. Vedaldi, and P. H. Torr, “Fully-convolutional siamese networks for object tracking,” in *European conference on computer vision*. Springer, 2016, pp. 850–865.
- [12] J. Liu, L. Song, and Y. Qin, “Prototype rectification for few-shot learning,” *arXiv preprint arXiv:1911.10713*, 2019.
- [13] Y. Xiao and R. Marlet, “Few-shot object detection and viewpoint estimation for objects in the wild,” *arXiv preprint arXiv:2007.12107*, 2020.
- [14] S. Ravi and H. Larochelle, “Optimization as a model for few-shot learning,” 2016.
- [15] C. Finn, P. Abbeel, and S. Levine, “Model-agnostic meta-learning for fast adaptation of deep networks,” *arXiv preprint arXiv:1703.03400*, 2017.
- [16] Z. Li, F. Zhou, F. Chen, and H. Li, “Meta-sgd: Learning to learn quickly for few-shot learning,” *arXiv preprint arXiv:1707.09835*, 2017.
- [17] A. Nichol, J. Achiam, and J. Schulman, “On first-order meta-learning algorithms,” *arXiv preprint arXiv:1803.02999*, 2018.
- [18] K. Lee, S. Maji, A. Ravichandran, and S. Soatto, “Meta-learning with differentiable convex optimization,” in *Proceedings of the IEEE Conference on Computer Vision and Pattern Recognition*, 2019, pp. 10 657–10 665.
- [19] O. Vinyals, C. Blundell, T. Lillicrap, D. Wierstra *et al.*, “Matching networks for one shot learning,” in *Advances in neural information processing systems*, 2016, pp. 3630–3638.
- [20] Y. Tian, Y. Wang, D. Krishnan, J. B. Tenenbaum, and P. Isola, “Rethinking few-shot image classification: a good embedding is all you need?” *arXiv preprint arXiv:2003.11539*, 2020.
- [21] D. Bahdanau, K. Cho, and Y. Bengio, “Neural machine translation by jointly learning to align and translate,” *arXiv preprint arXiv:1409.0473*, 2014.
- [22] M.-T. Luong, H. Pham, and C. D. Manning, “Effective approaches to attention-based neural machine translation,” *arXiv preprint arXiv:1508.04025*, 2015.
- [23] J. Gehring, M. Auli, D. Grangier, D. Yarats, and Y. N. Dauphin, “Convolutional sequence to sequence learning,” *arXiv preprint arXiv:1705.03122*, 2017.
- [24] A. Vaswani, N. Shazeer, N. Parmar, J. Uszkoreit, L. Jones, A. N. Gomez, Ł. Kaiser, and I. Polosukhin, “Attention is all you need,” in *Advances in neural information processing systems*, 2017, pp. 5998–6008.
- [25] X. Wang, R. Girshick, A. Gupta, and K. He, “Non-local neural networks,” in *Proceedings of the IEEE conference on computer vision and pattern recognition*, 2018, pp. 7794–7803.
- [26] H. Zhao, Y. Zhang, S. Liu, J. Shi, C. Change Loy, D. Lin, and J. Jia, “Psanet: Point-wise spatial attention network for scene parsing,” in *Proceedings of the European Conference on Computer Vision (ECCV)*, 2018, pp. 267–283.
- [27] J. Fu, J. Liu, H. Tian, Y. Li, Y. Bao, Z. Fang, and H. Lu, “Dual attention network for scene segmentation,” in *Proceedings of the IEEE Conference on Computer Vision and Pattern Recognition*, 2019, pp. 3146–3154.
- [28] Y. Cao, J. Xu, S. Lin, F. Wei, and H. Hu, “Gcnet: Non-local networks meet squeeze-excitation networks and beyond,” in *Proceedings of the IEEE International Conference on Computer Vision Workshops*, 2019, pp. 0–0.
- [29] H. Hu, Z. Zhang, Z. Xie, and S. Lin, “Local relation networks for image recognition,” in *Proceedings of the IEEE International Conference on Computer Vision*, 2019, pp. 3464–3473.
- [30] X. Zhu, D. Cheng, Z. Zhang, S. Lin, and J. Dai, “An empirical study of spatial attention mechanisms in deep networks,” in *Proceedings of the IEEE International Conference on Computer Vision*, 2019, pp. 6688–6697.
- [31] J. Hu, L. Shen, and G. Sun, “Squeeze-and-excitation networks,” in *Proceedings of the IEEE conference on computer vision and pattern recognition*, 2018, pp. 7132–7141.
- [32] M. Yin, Z. Yao, Y. Cao, X. Li, Z. Zhang, S. Lin, and H. Hu, “Disentangled non-local neural networks,” *arXiv preprint arXiv:2006.06668*, 2020.
- [33] H. Emami, M. M. Aliabadi, M. Dong, and R. B. Chinnam, “Spa-gan: Spatial attention gan for image-to-image translation,” *IEEE Transactions on Multimedia*, vol. 23, pp. 391–401, 2020.

- [34] J. Li, X. Liu, W. Zhang, M. Zhang, J. Song, and N. Sebe, “Spatiotemporal attention networks for action recognition and detection,” *IEEE Transactions on Multimedia*, vol. 22, no. 11, pp. 2990–3001, 2020.
- [35] D. Zhang, D. Meng, C. Li, L. Jiang, Q. Zhao, and J. Han, “A self-paced multiple-instance learning framework for co-saliency detection,” in *Proceedings of the IEEE international conference on computer vision*, 2015, pp. 594–602.
- [36] J. Han, G. Cheng, Z. Li, and D. Zhang, “A unified metric learning-based framework for co-saliency detection,” *IEEE Transactions on Circuits and Systems for Video Technology*, vol. 28, no. 10, pp. 2473–2483, 2017.
- [37] Q. Fan, D.-P. Fan, H. Fu, C.-K. Tang, L. Shao, and Y.-W. Tai, “Group collaborative learning for co-salient object detection,” in *Proceedings of the IEEE/CVF Conference on Computer Vision and Pattern Recognition*, 2021, pp. 12288–12298.
- [38] R. Girshick, J. Donahue, T. Darrell, and J. Malik, “Rich feature hierarchies for accurate object detection and semantic segmentation,” in *Proceedings of the IEEE conference on computer vision and pattern recognition*, 2014, pp. 580–587.
- [39] R. Girshick, “Fast r-cnn,” in *Proceedings of the IEEE international conference on computer vision*, 2015, pp. 1440–1448.
- [40] S. Ren, K. He, R. Girshick, and J. Sun, “Faster r-cnn: Towards real-time object detection with region proposal networks,” in *Advances in neural information processing systems*, 2015, pp. 91–99.
- [41] T.-Y. Lin, P. Dollár, R. Girshick, K. He, B. Hariharan, and S. Belongie, “Feature pyramid networks for object detection,” in *Proceedings of the IEEE conference on computer vision and pattern recognition*, 2017, pp. 2117–2125.
- [42] T.-Y. Lin, P. Goyal, R. Girshick, K. He, and P. Dollár, “Focal loss for dense object detection,” in *Proceedings of the IEEE international conference on computer vision*, 2017, pp. 2980–2988.
- [43] H. Law and J. Deng, “Cornernet: Detecting objects as paired keypoints,” in *Proceedings of the European Conference on Computer Vision (ECCV)*, 2018, pp. 734–750.
- [44] Z. Tian, C. Shen, H. Chen, and T. He, “Fcos: Fully convolutional one-stage object detection,” in *Proceedings of the IEEE international conference on computer vision*, 2019, pp. 9627–9636.
- [45] X. Zhou, D. Wang, and P. Krähenbühl, “Objects as points,” *arXiv preprint arXiv:1904.07850*, 2019.
- [46] H. Chen, Y. Wang, G. Wang, and Y. Qiao, “Lstd: A low-shot transfer detector for object detection,” *arXiv preprint arXiv:1803.01529*, 2018.
- [47] G.-J. Qi, X.-S. Hua, Y. Rui, T. Mei, J. Tang, and H.-J. Zhang, “Concurrent multiple instance learning for image categorization,” in *2007 IEEE Conference on Computer Vision and Pattern Recognition*. IEEE, 2007, pp. 1–8.
- [48] P. Dollár, B. Babenko, S. Belongie, P. Perona, and Z. Tu, “Multiple component learning for object detection,” in *European conference on computer vision*. Springer, 2008, pp. 211–224.
- [49] B. Babenko, M.-H. Yang, and S. Belongie, “Robust object tracking with online multiple instance learning,” *IEEE transactions on pattern analysis and machine intelligence*, vol. 33, no. 8, pp. 1619–1632, 2010.
- [50] X. Wang, T. E. Huang, T. Darrell, J. E. Gonzalez, and F. Yu, “Frustratingly simple few-shot object detection,” *arXiv preprint arXiv:2003.06957*, 2020.
- [51] J. Wu, S. Liu, D. Huang, and Y. Wang, “Multi-scale positive sample refinement for few-shot object detection,” *arXiv preprint arXiv:2007.09384*, 2020.
- [52] A. Paszke, S. Gross, S. Chintala, G. Chanan, E. Yang, Z. DeVito, Z. Lin, A. Desmaison, L. Antiga, and A. Lerer, “Automatic differentiation in pytorch,” 2017.
- [53] T.-Y. Lin, M. Maire, S. Belongie, J. Hays, P. Perona, D. Ramanan, P. Dollár, and C. L. Zitnick, “Microsoft coco: Common objects in context,” in *European conference on computer vision*. Springer, 2014, pp. 740–755.
- [54] M. Everingham, L. Van Gool, C. K. Williams, J. Winn, and A. Zisserman, “The pascal visual object classes (voc) challenge,” *International journal of computer vision*, vol. 88, no. 2, pp. 303–338, 2010.
- [55] R. Socher, M. Ganjoo, H. Sridhar, O. Bastani, C. D. Manning, and A. Y. Ng, “Zero-shot learning through cross-modal transfer,” *arXiv preprint arXiv:1301.3666*, 2013.



Tung-I Chen received the B.E. degree in the Department of Biomedical Engineering, National Cheng Kung University (NCKU) in 2019, and the M.S. degree in the Department of Computer Science & Information Engineering, National Taiwan University (NTU) in 2021. His research interests include computer vision, object detection and machine learning theory.



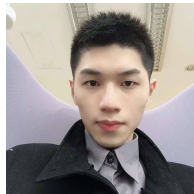
Yueh-Cheng Liu received M.S. degree from computer science department in National Taiwan University (NTU) in 2020. He is currently a research assistant in vision science lab in EE department at National Tsing Hua University. His research interests include computer vision, robotic learning, and 3D scene understanding.



Hung-Ting Su is currently pursuing the Ph.D. degree with the Graduated Institute of Networking and Multimedia, National Taiwan University, Taipei, Taiwan. His current research interests include multimodal comprehension and unsupervised learning.



Yu-Cheng Chang received his M.S. degree from the Department of Computer Science and Information Engineering, National Taiwan University, Taipei, Taiwan, in 2020. His research interests include machine learning and medical image processing.



Yu-Hsiang Lin received the M.S. degree in statistics from National Yang Ming Chiao Tung University, Hsinchu, Taiwan, in 2019. He is currently a research assistant at National Tsing Hua University, Taiwan. His research interests include object detection, natural language processing, sentiment analysis, and deep learning.



Jia-Fong Yeh received the B.S. degree and the M.S. degree in Computer Science and Information Engineering from National Taiwan Normal University (NTNU), Taiwan, in 2017 and 2019, respectively. He is currently pursuing his Ph.d. degree in Computer Science and Information Engineering at Natioal Taiwan University (NTU), Taiwan. His research interests include machine learning (ML), evolutionary algorithms (EAs), and computer games (CG). Recently, He is devoted to the study on few-shot learning. Jia-Fong is a student member of IEEE.



Winston H. Hsu (S'03–M'07–SM'12) received the Ph.D. degree in electrical engineering from Columbia University, New York, NY, USA. He is keen to realizing advanced researches towards business deliverables via academia-industry collaborations and co-founding startups. Since 2007, he has been a Professor with the Graduate Institute of Networking and Multimedia and the Department of Computer Science and Information Engineering, National Taiwan University. His research interests include large-scale image/video retrieval/mining, visual recognition, and machine intelligence. Dr. Hsu served as the Associate Editor for the IEEE TRANSACTIONS ON MULTIMEDIA and on the Editorial Board for the IEEE MultiMedia Magazine.